# Inclusion of temperature effects in a model of magnetoelasticity

Document Version:
Publisher's PDF, also known as Version of Record (includes final page, issue and volume numbers)

Please check the document version of this publication:

• A submitted manuscript is the version of the article upon submission and before peer-review. There can be important differences between the submitted version and the official published version of record. People interested in the research are advised to contact the author for the final version of the publication, or visit the DOI to the publisher's website.
• The final author version and the galley proof are versions of the publication after peer review.
• The final published version features the final layout of the paper including the volume, issue and page numbers.

[Link to publication](Link to publication)

Download date: 06. Feb. 2025

# Inclusion of Temperature Effects in a Model of Magnetoelasticity

T. Emilia Motoasca[1], Peter M. van den Berg[2], Hans Blok[3], and Martin D. Verweij[3]

[1]Faculty of Electrical Engineering, Eindhoven University of Technology, 5600 MB Eindhoven, The Netherlands
[2]Faculty of Applied Sciences, Delft University of Technology, 2628 CJ Delft, The Netherlands
[3]Faculty of Electrical Engineering, Mathematics and Computer Science, Delft University of Technology,
2628 CD Delft, The Netherlands

In this paper, we report on temperature effects associated with elastic electromagnetic forming by pulsed electromagnetic fields in inhomogeneous, linear, and lossy media. In a previous paper, we discussed the electromagnetic forces associated with these pulsed electromagnetic fields. Here, we calculate the temperature rise from the equation of heat flow in an isolated object to be deformed. The temperature rise is included in the elastodynamic problem to be solved for the presence of electromagnetic forces, and as a consequence the thermoelastic field can be obtained. As an example, we calculate the thermoelastic field in a hollow cylindrical object.

*Index Terms*—Conducting magnetic materials, elastic field, electromagnetic forming, electromechanical forces, temperature rise, thermoelastic field.

## I. INTRODUCTION

**T**HE subject of a vast and sometimes controversial literature, [1]–[8], is how the forces in electromagnetic bodies describe the so-called electromagnetic forming, a process of shaping metal objects using pulsed electromagnetic fields. Development of an accurate theoretical model of this process is not trivial, since we have to use a complete physical system to describe the motion of a continuum (the object to be shaped, the so-called workpiece) under the influence of a strong electromagnetic field, that is generated by a forming coil. According to Penfield and Haus [9], this complete physical system consists of three mutually coupled subsystems: a mechanical subsystem describing the mechanics of the moving material masses; an electromagnetic subsystem describing the dynamics of the electromagnetic fields; and a thermodynamic subsystem taking into account the internal energy and the generation of heat and its flow.

The mechanical subsystem and the electromagnetic subsystem have been investigated in [10]. There, the electromechanical force densities associated with pulsed electromagnetic fields in piecewise homogeneous, isotropic, linear, and lossy media have been discussed. It has been shown that the conductivity and the gradients in permittivity and in permeability lead to volume force densities, while jump discontinuities in permittivity and permeability lead to surface force densities. These electromagnetic force densities acted as volume (body) source densities in the elastodynamic equations and as surface source densities in the corresponding boundary conditions that govern the elastic and anelastic motion of deformable matter. The theory developed has been applied to a practical configuration consisting of a hollow cylindrical domain with a high electrical conductivity (representing the workpiece) placed inside a cylindrical sheet antenna (repre-

senting the forming coil) carrying a given electric current per unit length. The configuration has been assumed to have infinite length and to be axially symmetric. It has been shown that the values of the electromagnetic volume force density are much larger in a magnetic material than in a nonmagnetic one and that the electromagnetic force density decays rapidly in time and space. Moreover, it has been shown that the theory of equivalent surface forces that was used by other authors [12]–[15], in describing electromagnetic forming does not take correctly into account the magnetic nature of the object (workpiece). As a result, within the linear approximation, the theory of equivalent surface sources leads to incorrect elastic deformations.

In the present paper, we continue the development of the theoretical model of an electromagnetic forming process and we introduce the thermodynamic subsystem, as being the third coupled subsystem described by Penfield and Haus in [9]. In the literature pertaining to electromagnetic forming, i.e., [11]–[15], it is generally assumed that the electromagnetic forming process is very short and hence there is no generation of heat or heat flow in the electromagnetic forming system. However, we consider that both the generation of heat and the heat flow have to be taken into account if our aim is a complete theoretical model of an electromagnetic forming process. If the effects of heat generation and heat flow show to be negligible, we may then neglect them in a simplified model of an electromagnetic forming process. In addition, in this simplified model, we only consider the elastic deformations. If this is not the case, we have to include all these effects in an improved model of electromagnetic forming.

In this paper, we describe the possible effects of heat generation and heat flow in the electromagnetic forming system that has been used as an example in [10]. The temperature distribution in the workpiece is then calculated in the assumption of an insulated workpiece. This temperature rise is introduced as an extra term in the elastodynamic solution presented in [10] and the thermoelastic field for a workpiece with linear elastodynamic properties is calculated. The components of the ther-

moelastic field are compared with the components of the elastic field and the effects of the temperature rise are discussed. We will show that the temperature rise has negative consequences for the electromagnetic compression, because in all cases a significant undesired expansion of the workpiece is obtained. This undesired expansion due to the temperature rise should disappear when the workpiece cools down, but it may have negative consequences in the forming system, i.e., deformation of the forming coil.

## II. EFFECTS OF HEAT GENERATION AND OF HEAT FLOW IN AN ELECTROMAGNETIC FORMING SYSTEM

All parts of an electromagnetic forming system play a role in the forming process, but here only the parameters related to the forming coil and the workpiece are investigated.

We consider an axially symmetric configuration consisting of a hollow cylindrical domain with a high electrical conductivity (representing the workpiece) placed inside a cylindrical sheet antenna (representing the forming coil) carrying a given electric current per unit length. The configuration has been assumed to have infinite length. In such a configuration, the temperature will have a certain distribution in the forming coil and in the workpiece as a result of the heat conduction and also as a result of the heat exchange between the components of the forming system and the environment.

The temperature rise may lead to changes in the geometry and in the material properties both in the forming coil and in the workpiece. In a reasonable range of temperatures, we may assume that the electromagnetic, elastic, and thermal properties of the materials in the forming coil and in the workpiece show a linear variation with temperature, hence we do not consider inelastic behavior of the workpiece.

The geometry of both the forming coil and workpiece changes within the forming process, not only due to the influence of electromagnetic forces, but also due to the temperature rise in the configuration. These changes in geometry due to a temperature rise concern linear dimensions, surface area, and volume, but only one type of geometric change is predominant in each configuration.

## III. TEMPERATURE DISTRIBUTION

We present here the evolution of the temperature in the workpiece due to dissipation of electromagnetic energy during the forming process. The configuration in which the temperature distribution will be determined is presented in Fig. 1. The position in the configuration is specified by the coordinates $\{r, \varphi, z\}$ with respect to the reference frame with the origin $\mathcal{O}$ and the three mutually perpendicular vectors $\{\boldsymbol{i}_r, \boldsymbol{i}_\varphi, \boldsymbol{i}_z\}$ of unit length each. In the indicated order, the base vectors form a right-handed system.

The temperature distribution in the workpiece during the electromagnetic forming process depends on the heat exchange between the forming coil and the workpiece, and the dissipation of electromagnetic energy in the workpiece itself (Joule losses). We expect that the major contribution to the temperature rise in the workpiece is due to the internal heat dissipation. So, in order to get an idea of the thermoelastic effects that correspond to such a rise, we have chosen for a model in which only the internal
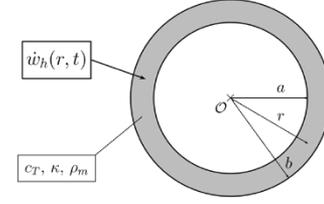


Fig. 1.   Cross section of the cylindrical configuration for the calculation of the temperature distribution that has as its source the known rate of heat dissipation.

heat dissipation will be taken into account. We will compute the temperature distribution in the workpiece, assuming that the boundaries of the workpiece are insulated. The latter assumption might lead to a somewhat too high temperature distribution, but that can partly compensate the neglected transfer of heat from the forming coil.

The source that excites the temperature field is the rate of energy generation in the workpiece $\dot{w}_h$ represented by the Joule losses inside the workpiece. The Joule losses may be inferred from the known values of the electromagnetic field components calculated in [10].

In the chosen cylindrical coordinate system, the equations governing the thermal state of the workpiece, namely the equation of heat flow and the thermal conduction equation are written as

$$\frac{1}{r}\partial_r(rq_r) + \rho_m c_T \partial_t T = \dot{w}_h \tag{1}$$

and

$$q_r = -\kappa \partial_r T \tag{2}$$

where $T$ is the temperature, $\rho_m$ is the mass density, $c_T$ is the specific heat, $\kappa$ is the thermal conductivity, and $q_r$ is the heat flow density (heat flux) in the radial direction. The source term $\dot{w}_h$ in the right-hand side of (1) represents the rate of volume density of the Joule losses in the workpiece

$$\dot{w}_h(r, t) = \sigma E_\varphi^2(r, t) \tag{3}$$

where $\sigma$ is the electrical conductivity. $E_\varphi(r, t)$ is the only nonzero component of the electric field and it has been calculated in [10]. Combining (1) and (2) results into

$$\partial_r^2 T + \frac{1}{r}\partial_r T - \frac{\rho_m c_T}{\kappa}\partial_t T = -\frac{1}{\kappa}\dot{w}_h. \tag{4}$$

This equation must be supplemented by the initial condition and the boundary conditions. The initial temperature within the whole configuration is $T_0$. For convenience, we will from now on consider the temperature $T(r, t)$ in (4) to be $T(r, t) - T_0$. That means that the initial condition for the temperature will be

$$\lim_{t \downarrow 0} T(r, t) = 0. \tag{5}$$

We have chosen here an insulated surface of the object, thus the heat flux is zero at the boundaries. As a result, we then have as boundary conditions

$$\lim_{r \downarrow a} \partial_r T(r, t) = 0,$$
$$\lim_{r \uparrow b} \partial_r T(r, t) = 0. \tag{6}$$

The simplest way to construct solutions to (4) that satisfy the proper boundary and excitation conditions and ensure causality is to use the Laplace transformation with respect to time. To illustrate the notation, let

$$\hat{T}(r,s) = \int_{t=0^-}^{\infty} \exp(-st)T(r,t)\,\mathrm{d}t \qquad (7)$$

where it has been assumed that the rate of volume density of the Joule losses in the workpiece $\dot{w}_h(r,t)$ starts to act at the instant $t = 0$. The complex transform parameter $s$ is taken in the right half of the complex $s$-plane. The Laplace transformed quantities are denoted with a hat symbol and we omit the explicit $s$-dependence in our notation. We take the limit $s \to j\omega$, so that we end up with the Fourier transformed quantities, where j is the imaginary unit and $\omega = 2\pi f$ is the radial frequency, while $f$ denotes the frequency of operation. After the application of the Laplace transform, (4) becomes

$$\partial_r^2 \hat{T} + \frac{1}{r}\partial_r \hat{T} - \gamma^2 \hat{T} = -\frac{1}{\kappa}\hat{\dot{w}}_h \qquad (8)$$

where $\gamma = \sqrt{s\rho_m c_T/\kappa}$.

We may write the total solution of (8) as

$$\hat{T}(r) = \hat{T}^{\mathrm{part}}(r) + \hat{T}^{\mathrm{gen}}(r) \qquad (9)$$

where $\hat{T}^{\mathrm{part}}(r)$ denotes the particular solution of (8) and $\hat{T}^{\mathrm{gen}}(r)$ denotes the general solution of the homogeneous form of (8).

The particular solution $\hat{T}^{\mathrm{part}}(r)$ is calculated using the Green's function $\hat{G}(r,r')$ as follows:

$$\hat{T}^{\mathrm{part}}(r) = \frac{1}{\kappa}\int_{r'=a}^{b}\hat{G}(r,r')\hat{\dot{w}}_r r'\,\mathrm{d}r' \qquad (10)$$

where $\hat{G}(r,r')$ is the solution of equation

$$\frac{1}{r}\partial_r(r\partial_r\hat{G}) - \gamma^2\hat{G} = -\frac{1}{r'}\delta(r-r') \qquad (11)$$

with the appropriate boundary and excitation conditions. We obtain

$$\hat{G}(r,r') = \begin{cases} I_0(\gamma r)K_0(\gamma r'), & \text{for } r \le r', \\ K_0(\gamma r)I_0(\gamma r'), & \text{for } r \ge r' \end{cases}. \qquad (12)$$

For $\gamma \to 0$, the limit of (10) is $\infty$, and we have to find a way to evaluate the integral in (10). We notice that we can also calculate the integral

$$\gamma^2\hat{T}^{\mathrm{part}}(r) = \frac{1}{\kappa}\int_{r'=a}^{b}\gamma^2\hat{G}(r,r')\hat{\dot{w}}_h(r')r'\,\mathrm{d}r' \qquad (13)$$

or

$$s\hat{T}^{\mathrm{part}}(r) = \frac{1}{\rho_m c_T}\int_{r'=a}^{b}\gamma^2\hat{G}(r,r')\hat{\dot{w}}_h(r')r'\,\mathrm{d}r'. \qquad (14)$$

The quantity $\hat{\dot{w}}_h(r')$ at the right-hand side of the above equation is a known quantity in the frequency domain and $\gamma^2\hat{G}(r,r')$ remains finite, so the integral may easily be evaluated. Its time-domain counterpart can be calculated using an inverse fast Fourier transform (FFT). Further, taking into account that

$$\frac{1}{s}F(s) \to \int_{\tau=0}^{t} f(\tau)\,\mathrm{d}\tau \qquad (15)$$

we can calculate the time-domain counterpart of $\hat{T}^{\mathrm{part}}(r)$ and then the values obtained can be transformed back to frequency domain. In our further analysis, we also need the radial derivative of the particular solution. This is obtained as

$$\partial_r\hat{T}^{\mathrm{part}}(r) = \frac{1}{\kappa}\int_{r'=a}^{b}\partial_r\hat{G}(r,r')\hat{\dot{w}}_h(r')r'\,\mathrm{d}r'. \qquad (16)$$

A special case in the calculation of the Green's function is represented by $\gamma \to 0(f \to 0)$. For this case, we have

$$\lim_{\gamma\to 0}\partial_r\hat{G}(r,r') = \begin{cases} 0, & \text{for } r < r' \\ -1/(2r), & \text{for } r = r' \\ -1/r, & \text{for } r > r' \end{cases}. \qquad (17)$$

The general solution $\hat{T}^{\mathrm{gen}}(r)$ of (8) is given by

$$\hat{T}^{\mathrm{gen}}(r) = CI_0(\gamma r) + DK_0(\gamma r) \qquad (18)$$

where the coefficients $C$ and $D$ are obtained from the boundary conditions

$$\lim_{r\downarrow a}\partial_r\hat{T}^{\mathrm{gen}} = -\partial_r\hat{T}^{\mathrm{part}}(a) = h(a),$$
$$\lim_{r\uparrow b}\partial_r\hat{T}^{\mathrm{gen}} = -\partial_r\hat{T}^{\mathrm{part}}(b) = h(b) \qquad (19)$$

with $\partial_r\hat{T}^{\mathrm{part}}$ from (16). Thus, the coefficients $C$ and $D$ may be calculated as

$$C = \frac{1}{\gamma}\frac{K_1(\gamma b)h(a) - K_1(\gamma a)h(b)}{I_1(\gamma a)K_1(\gamma b) - K_1(\gamma a)I_1(\gamma b)},$$
$$D = \frac{1}{\gamma}\frac{I_1(\gamma b)h(a) - I_1(\gamma a)h(b)}{I_1(\gamma a)K_1(\gamma b) - K_1(\gamma a)I_1(\gamma b)}. \qquad (20)$$

With the particular solution $\hat{T}^{\mathrm{gen}}(r)$ in (10) and with the general solution $\hat{T}^{\mathrm{gen}}(r)$ in (18), the solution for $\hat{T}$ in (9) is obtained. The results for the temperature field $\hat{T}$ may then be transformed back to time domain using an inverse FFT.

*Isothermal Case for a Thin Workpiece:* When the workpiece is very thin and we assume that it has the same temperature at every location, the calculation of the temperature distribution may be simplified since the heat flux, $q_r = 0$, and we then have from (1)

$$\hat{T}(r) = \frac{1}{\gamma^2\kappa}\hat{\dot{w}}_h. \qquad (21)$$

Further, a first estimate of the temperature of the workpiece may be obtained using the approximation of Joule losses $\dot{w}_h$ in the workpiece with the network model

$$\dot{w}_h(t) = \frac{I_S^2(t)}{\sigma(b-a)^2} \qquad (22)$$

in which $I_S$ denotes the electric current in the forming coil per unit length along the cylindrical direction. Since the Joule losses are totally converted into heat, in this case the actual temperature of the workpiece will be

$$T(t) = \frac{1}{\rho_m c_T \sigma(b-a)^2}\int_{\tau=0}^{t} I_S^2(\tau)\,\mathrm{d}\tau. \qquad (23)$$

Since this temperature holds in the entire workpiece, the mean temperature $T_{\mathrm{mean}}(t)$ of the workpiece equals

$$T_{\mathrm{mean}}(t) = T(t). \qquad (24)$$

## IV. THERMOELASTIC FIELD IN THE WORKPIECE

This section presents the calculation of the thermoelastic field in the infinite, hollow, cylindrical, conducting object in Fig. 1. The configuration is locally excited by the electromagnetic volume and surface force densities calculated in [10], together with the temperature rise in the object, calculated in Section III. The equations of the thermoelastic field for a workpiece with linear elastodynamic properties [21] are

$$\partial_r \tau_{rr} + \frac{\partial_\varphi \tau_{r\varphi}}{r} + \partial_z \tau_{rz} + \frac{\tau_{rr} - \tau_{\varphi\varphi}}{r} - \rho_m \partial_t^2 u_r = -f_r^V,$$
$$\partial_r \tau_{r\varphi} + \frac{\partial_\varphi \tau_{\varphi\varphi}}{r} + \partial_z \tau_{\varphi z} + \frac{\tau_{r\varphi}}{r} - \rho_m \partial_t^2 u_\varphi = 0,$$
$$\partial_r \tau_{rz} + \frac{\partial_\varphi \tau_{\varphi z}}{r} + \partial_z \tau_{zz} + \frac{\tau_{rz}}{r} - \rho_m \partial_t^2 u_z = 0 \qquad (25)$$

where $f_r^V$ is the electromagnetic volume force density. The boundary conditions to be applied at $r = a$ and $r = b$ are

$$\lim_{r \downarrow a} \tau_{rr}(r,t) = -f_r^S(a,t),$$
$$\lim_{r \uparrow b} \tau_{rr}(r,t) = f_r^S(b,t) \qquad (26)$$

where $f_r^S(a,t)$ and $f_r^S(b,t)$ are the electromagnetic surface force densities at the boundaries $r = a$ and $r = b$, respectively.

We consider the plane-strain case where the nonzero thermoelastic normal strains are defined as

$$e_{rr} = \partial_r u_r, \quad e_{\varphi\varphi} = r^{-1} u_r \qquad (27)$$

and the constitutive relations (see [21]) are

$$\tau_{rr} = (\lambda_L + 2\mu_L)e_{rr} + \lambda_L e_{\varphi\varphi} + \lambda_L e_{zz} - \beta T,$$
$$\tau_{\varphi\varphi} = \lambda_L e_{rr} + (\lambda_L + 2\mu_L)e_{\varphi\varphi} + \lambda_L e_{zz} - \beta T,$$
$$\tau_{zz} = \lambda_L e_{rr} + \lambda_L e_{\varphi\varphi} + (\lambda_L + 2\mu_L)e_{zz} - \beta T \qquad (28)$$

where $\beta = \alpha_T(3\lambda_L + 2\mu_L)$ and $\alpha_T$ is the coefficient of linear thermal expansion of the workpiece (see [21]). We will focus here on solving the equation of motion in the radial direction. This equation is obtained from (25) when applying the constitutive relations in (28). After the application of the Laplace transform with $s \to j\omega$ to (25), the following equation of motion in the radial direction results:

$$\partial_r^2 \hat{u}_r + \frac{1}{r}\partial_r \hat{u}_r - \frac{1}{r^2}\hat{u}_r + k^2 \hat{u}_r = -\frac{\hat{f}_r^V - \beta\,\partial_r\hat{T}}{\lambda_L + 2\mu_L} \qquad (29)$$

where $k = \omega/c_P$ is the wavenumber. This equation can be solved in a similar manner as in [10], since $T$ is a known quantity, calculated as in Section III. We write the total solution of (29) as

$$\hat{u}_r(r) = \hat{u}_r^{\text{part}}(r) + \hat{u}_r^{\text{gen}}(r) \qquad (30)$$

where $\hat{u}_r^{\text{part}}(r)$ denotes the particular solution of (29) and $\hat{u}_r^{\text{gen}}(r)$ denotes the general solution of the homogeneous form of (29).
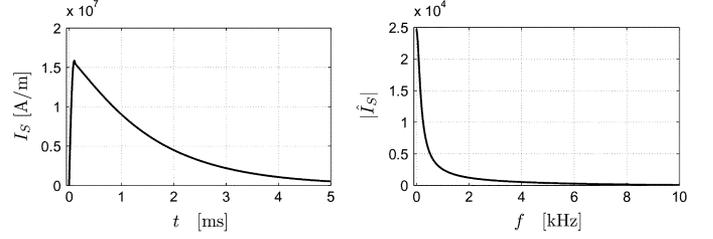


Fig. 2.   Current per unit length in the sheet antenna.

Hence, the solution for $\hat{u}_r$ is obtained as

$$\hat{u}_r(r) = \hat{u}_r^{\text{part}}(r) + J_1(kr)\frac{N(kb)h(a) - N(ka)h(b)}{M(ka)N(kb) - N(ka)M(kb)}$$
$$+ Y_1(kr)\frac{-M(kb)h(a) + M(ka)h(b)}{M(ka)N(kb) - N(ka)M(kb)} \qquad (31)$$

with

$$M(kr) = k(\lambda_L + 2\mu_L)J_0(kr) - \frac{2\mu_L}{r}J_1(kr),$$
$$N(kr) = k(\lambda_L + 2\mu_L)Y_0(kr) - \frac{2\mu_L}{r}Y_1(kr) \qquad (32)$$

and

$$h(a) = -\hat{f}_r^S(a) - \hat{\tau}_{rr}^{\text{part}}(a),$$
$$h(b) = \hat{f}_r^S(b) - \hat{\tau}_{rr}^{\text{part}}(b). \qquad (33)$$

Now, all nonzero components of the strain and stress tensor may be calculated in the frequency domain and then be transformed back to time domain using an inverse FFT.

## V. NUMERICAL RESULTS

In this section, we present some numerical results for typical electromagnetic forming systems designed for compression of hollow circular cylindrical workpieces. The workpiece subjected to electromagnetic compression has an inner radius $r = a = 20$ mm and an outer radius $r = b = 22$ mm. With this geometry two types of materials have been chosen, one nonmagnetic ($\mu = \mu_0$) and one hypothetical linear magnetic material ($\mu = 100\mu_0$). In both cases, the electrical conductivity of the workpiece is $\sigma = 3.6 \cdot 10^7$ S/m and the forming coil is a cylindrical current sheet located at $r = c = 24$ mm. The current per unit length $I_S(t)$ flowing in the sheet antenna is the same damped pulse used in [10]; see Fig. 2.

Further, in both cases, the workpiece has the same elastic properties and it has a linear elastic behavior within the whole range of stresses and strains. The workpiece has the Lamé coefficients of elasticity $\lambda_L = 17 \cdot 10^{10}$ N/m$^2$, $\mu_L = 8 \cdot 10^{10}$ N/m$^2$, a specific heat $c_T = 880$ J/(kg K), a thermal conductivity $\kappa = 190$ W/(m K), and a mass density $\rho_m = 2.7 \cdot 10^3$ kg/m$^3$. The coefficient of linear thermal expansion is $\alpha_T = 12.6 \cdot 10^{-6}$ K$^{-1}$.

We first compute the temperature distribution in the workpiece in the space-time domain. Also, the evolution in the time domain of the mean temperature $T_{\text{mean}}$ is presented. The mean temperature $T_{\text{mean}}$ in the workpiece has been calculated in two ways, as the average of the temperature distribution over the thickness of the workpiece, and as the mean temperature in the absence of thermal conduction inside the workpiece. The
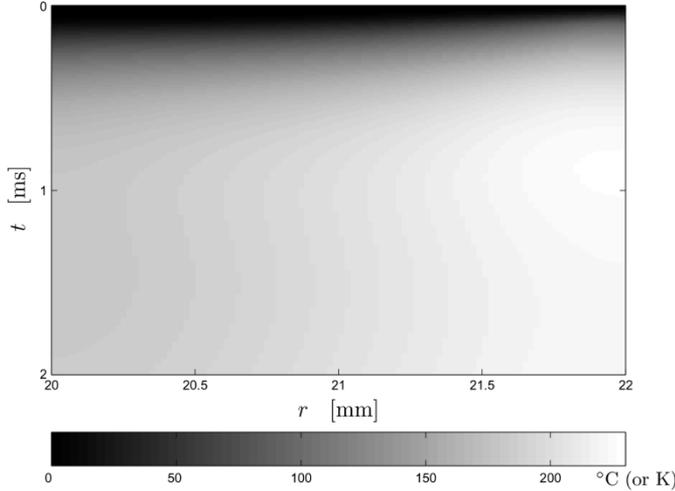
Fig. 3. Temperature rise $T$ in space-time domain for a nonmagnetic ($\mu = \mu_0$) workpiece.
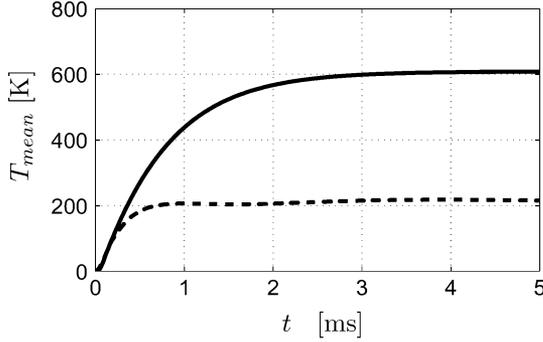


Fig. 5. Temperature rise $T$ in space-time domain for a magnetic ($\mu = 100\,\mu_0$) workpiece.



Fig. 4. Mean temperature $T_{\text{mean}}$ in the time domain, obtained from the exact results (solid lines) and obtained from neglecting thermal conduction (dashed lines) for a nonmagnetic ($\mu = \mu_0$) workpiece.



Fig. 6. Mean temperature $T_{\text{mean}}$ in the time domain, obtained from the exact results (solid lines) and obtained from neglecting thermal conduction (dashed lines) for a magnetic ($\mu = 100\,\mu_0$) workpiece.

latter approach is considered to be a good approximation for a thin workpiece; see (24). Subsequently the thermoelastic field is calculated.

In particular, we will present results for the radial displacement $u_r$, the radial strain $\varepsilon_r = \varepsilon_{rr}$, the tangential strain $\varepsilon_\varphi = \varepsilon_{\varphi\varphi}$, the radial stress $\sigma_r = \tau_{rr}$, the tangential stress $\sigma_\varphi = \tau_{\varphi\varphi}$, and the longitudinal stress $\sigma_z = \tau_{zz}$ and a comparison of these results with the elastodynamic field calculated in [10].

*Temperature Results:* In Figs. 3 and 4 we present the space-time evolution of the temperature and the temporal evolution of the mean temperature, respectively, in a nonmagnetic thick workpiece subjected to compression, while in Figs. 5 and 6, the same quantities in a magnetic thick workpiece subjected to compression are presented.

We also present in Figs. 4 and 6 the results for the mean temperature for a very thin workpiece, where we neglect the thermal conduction (dashed lines), using (23)–(24).

We notice that in all cases under consideration, the temperature has large values. For the nonmagnetic and the magnetic thick workpieces, the temperature rise reaches values at which the workpiece will melt. However, the calculated values do not take into account the heat exchange with the surrounding medium.
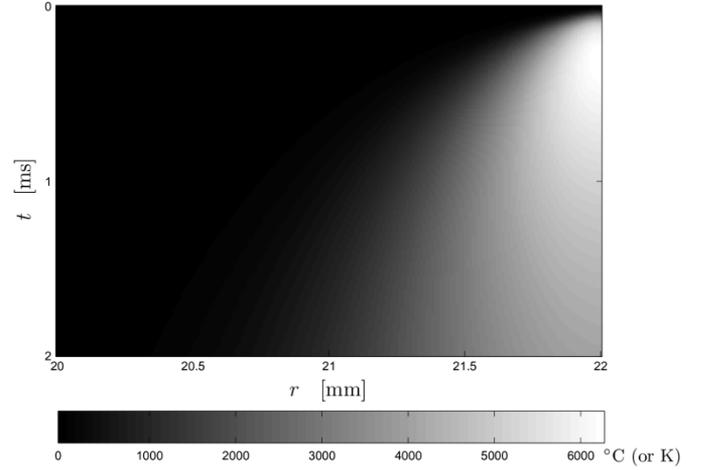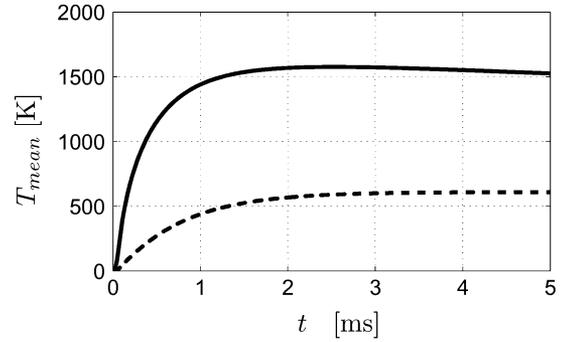
*Thermoelastic Results:* With the known evolution of the temperature within the workpiece, calculated in Section V, the evolution of the thermoelastic field has been calculated as well, using the method described in Section VI.

In Fig. 7, the nonzero components of the elastic field and of the thermoelastic field, $u_r, \varepsilon_r, \varepsilon_\varphi, \sigma_r, \sigma_\varphi$, and $\sigma_z$ in the time domain at $r = a$ are presented.

With the chosen elastic and thermal properties of the material, we notice that the influence of temperature rise on the elastic field components (except $\sigma_r$) is rather small in the beginning of the time interval of analysis (when $t < 0.1$ ms). In this time interval the temperature rise is small, thus the effect of the temperature terms in the thermoelastic field is small.

The temperature rise affects the values of the radial displacement $u_r$ in a significant way, since at the end of the considered time interval we have an expansion of the inner boundary $r = a$ while the intention of the process is to reach a compression of it. The strains $\varepsilon_r$ and $\varepsilon_\varphi$ are affected by the temperature rise in the same way as the radial displacement $u_r$.

The values of the tangential stress $\sigma_\varphi$ for the thermoelastic case are smaller than the corresponding values for the elastic case, but still this is the most significant stress component. Due to the temperature rise in the workpiece, the values of radial stress $\sigma_r$ in the thermoelastic case are much larger than the corresponding negligible values for the elastic case. However, the
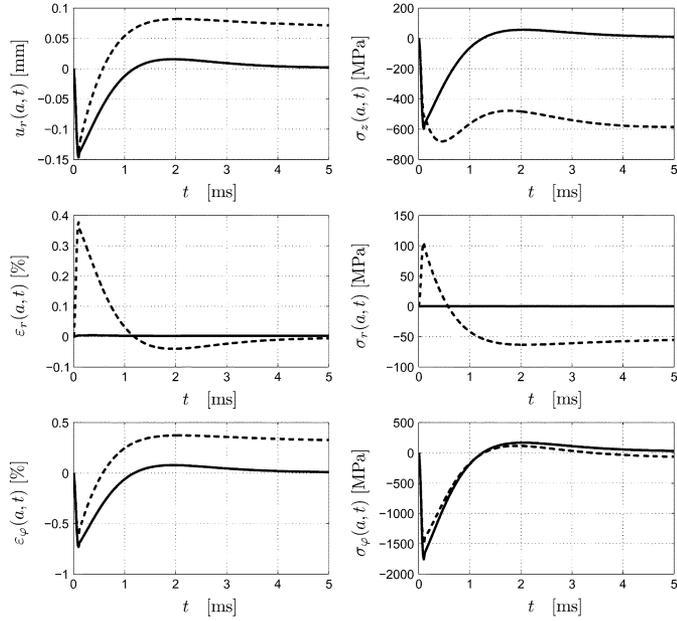
Fig. 7.  Elastic (solid lines) and thermoelastic (dashed lines) field components at $r = a$ in the time domain for the nonmagnetic ($\mu = \mu_0$) workpiece.

absolute values of the radial stress $\sigma_r$ in the thermoelastic case are about ten times smaller than the absolute values of the tangential stress $\sigma_\varphi$ in the same case, thus they can be neglected. For the thermoelastic case, the longitudinal stress $\sigma_z$ has negative values that are about three times smaller than the values of the tangential stress $\sigma_\varphi$ and it cannot be neglected in further calculations.

The most important component of the elastic and of the thermoelastic field is the radial displacement $u_r$, since in electromagnetic forming we would like to achieve a certain deformation of the workpiece. Therefore, the space-time evolution of the radial displacement $u_r$ in a nonmagnetic ($\mu = \mu_0$) thick ($b - a = 2$ mm) workpiece subjected to compression is presented in Fig. 8, both for the elastic case and for the thermoelastic case.

Since the temperature effect is small, for $t < 0.1$ ms in the thermoelastic case, the radial displacement $u_r(r, t)$ is still negative (indicating a compression), but its absolute values are smaller than the corresponding values in the elastic case. For $t > 1$ ms, in the thermoelastic case, the radial displacement $u_r(r, t)$ reaches positive values, indicating an expansion of the workpiece. This expansion is in the same order of magnitude with the compression obtained for $t < 1$ ms. The intention of the electromagnetic forming process under consideration is to obtain only the compression of the workpiece, but due to the temperature rise we will obtain also an undesired expansion of the workpiece.

Therefore, in this case the temperature rise may be seen as a negative consequence that affects the deformation process. This negative effect should disappear at the end of the process when the workpiece cools down as an effect of the heat exchange with the environment.

In Fig. 9, the nonzero components of the elastic field and of the thermoelastic field, $u_r, \varepsilon_r, \varepsilon_\varphi, \sigma_r, \sigma_\varphi$, and $\sigma_z$, at $r = a$ in
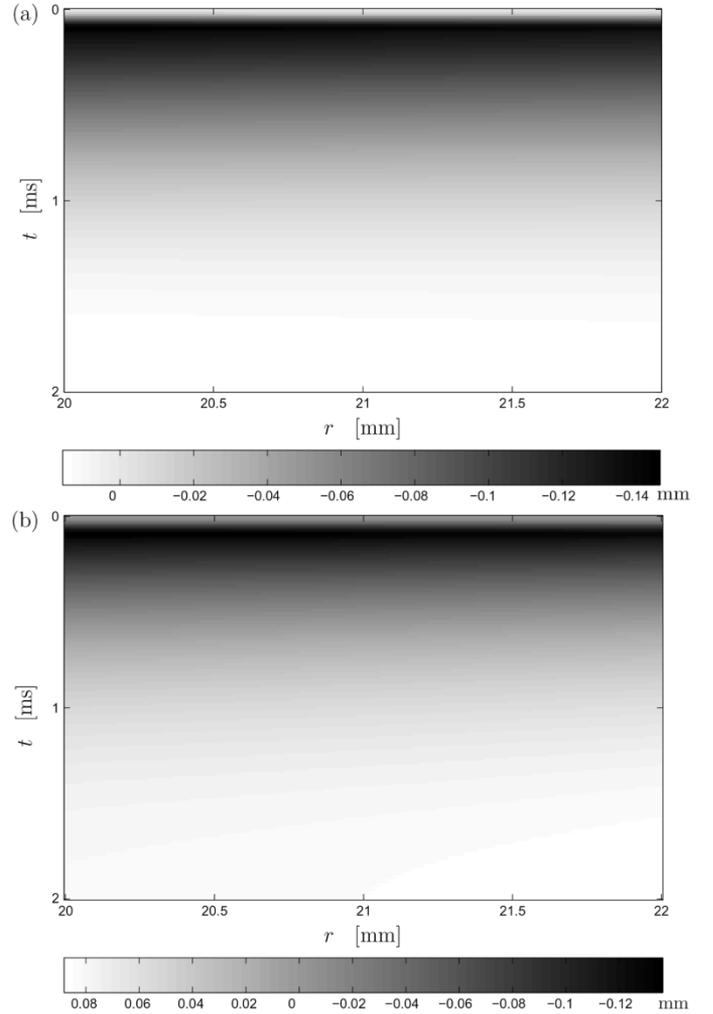


Fig. 8.  Radial displacement $u_r$ in space-time domain for the nonmagnetic ($\mu = \mu_0$) workpiece calculated from (a) the elastic field and (b) the thermoelastic field.

a magnetic ($\mu = 100\mu_0$) thick ($b - a = 2$ mm) workpiece subjected to compression are presented.

The temperature effect on the radial displacement $u_r(a, t)$ is small at the beginning of the time interval, but then it becomes significant. In the same manner as for the nonmagnetic workpiece, at the end of the considered time interval the radial displacement becomes positive, indicating expansion at the inner boundary of the workpiece.

The temperature rise also affects the values of the strains $\varepsilon_r$ and $\varepsilon_\varphi$. When temperature effects are taken into account, $\varepsilon_r$ very quickly reaches negative values, while in simple elastic field calculation it had only positive values during the whole time interval of observation. The same remark is valid for the radial stress $\sigma_r$. When temperature effects are taken into account, $\varepsilon_\varphi$ very quickly reaches positive values, while in simple elastic field calculation it has only negative values during the whole time interval of observation. The same remark is valid for the tangential stress $\sigma_\varphi$ and for the longitudinal stress $\sigma_z$.

The space-time evolution of the radial displacement $u_r$ in a magnetic ($\mu = 100\mu_0$) thick ($b - a = 2$ mm) workpiece subjected to compression is presented in Fig. 10, both for
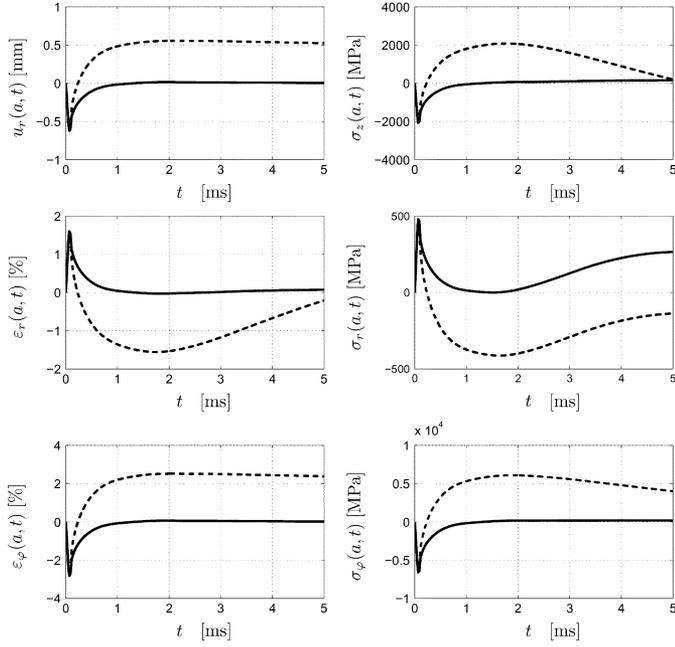
Fig. 9. Elastic (solid lines) and thermoelastic (dashed lines) field components at $r = a$ in the time domain for the magnetic ($\mu = 100\mu_0$) workpiece.



Fig. 10. Radial displacement $u_r$ in space-time domain for the magnetic ($\mu = 100\mu_0$) workpiece calculated from (a) the elastic field and (b) the thermoelastic field.

the elastic case and for the thermoelastic case. The radial displacement $u_r$ in the thermoelastic case reaches positive values in a short interval of time $t > 1$ ms. This positive radial displacement $u_r$ (indicating expansion of the workpiece) is in the same order of magnitude with the absolute value of the negative displacement at the beginning of the time interval. Also for the magnetic workpiece, the temperature rise may be seen as a negative consequence that affects the deformation process and the unwanted expansion should disappear at the end of the process when the workpiece cools down as an effect of the heat exchange with the environment. For the magnetic workpiece under consideration, the unwanted expansion at the end of the considered time interval is considerably larger than for a nonmagnetic workpiece.

## VI. CONCLUSION

A theoretical model of an electromagnetic forming process requires a description of three mutually coupled subsystems: a mechanical subsystem describing the mechanics of the moving material masses, an electromagnetic subsystem describing the dynamics of the electromagnetic fields, and a thermodynamic subsystem taking into account the internal energy and the generation of heat and its flow. In addition to the previous work wherein the coupled mechanical subsystem and the electromagnetic subsystem have been discussed [10] we have included in the model the thermodynamic subsystem, as the third coupled subsystem describing the motion of a continuum (the object to be shaped, the so-called workpiece) under the influence of a strong electromagnetic field.

In general, the possible effects of heat generation and heat flow in an electromagnetic forming system have been presented. The changes in the ge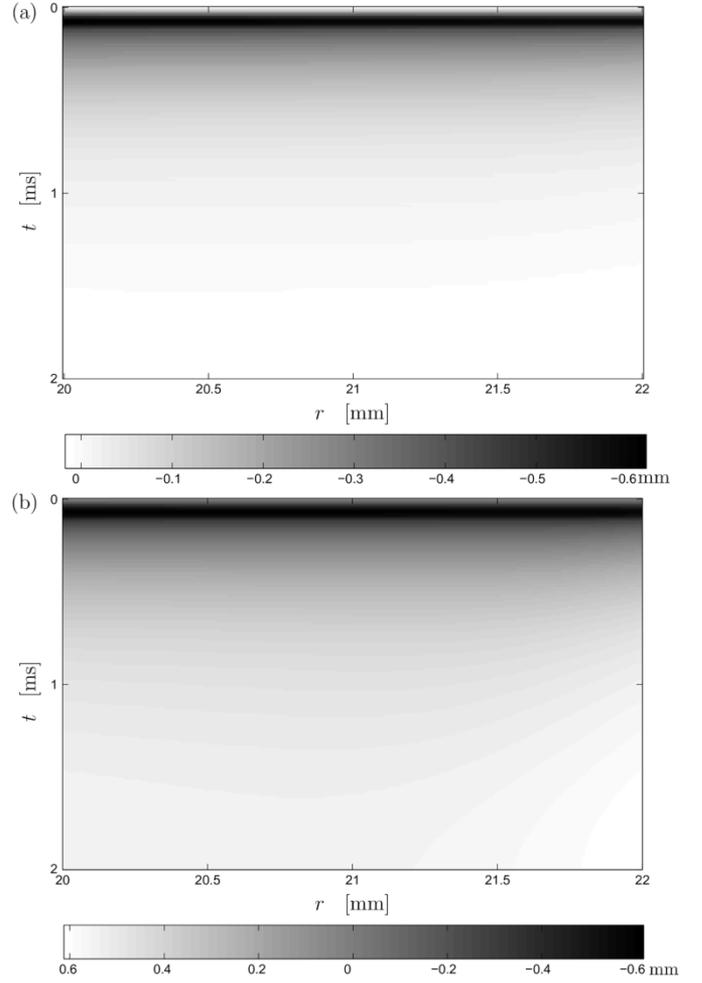ometry and in the physical properties of all the forming devices have been restricted to the most important devices, the forming coil and the workpiece.

The axially symmetric configuration consisted of a hollow cylindrical domain with a high electrical conductivity (representing the workpiece) placed inside a cylindrical sheet antenna (representing the forming coil) carrying a given electric current per unit length. The configuration has been assumed to have infinite length and it is a good model for electromagnetic compression. The temperature distribution in the workpiece has been calculated in the assumption of an insulated workpiece. The temperature rise is due to the dissipation of electromagnetic energy, dissipation that is in fact the volume density of the Joule losses.

The temperature distribution was then introduced as an extra term in the elastodynamic solution presented in [10] and the thermoelastic field was calculated. A comparison of the nonzero components of the elastic and thermoelastic field components has shown that in the present case of electromagnetic compression, the temperature rise may lead to an unwanted expansion. It has been shown that for a magnetic workpiece this unwanted expansion is much larger than for the case of a nonmagnetic workpiece. This unwanted expansion should disappear at the end of

the deformation process when the heat exchange with the environment has been completed.

However, on a similar model for electromagnetic expansion the temperature rise will produce an supplementary expansion of the workpiece, thus the temperature rise is favorable for electromagnetic expansion.

We mention that here only the elastic deformations with a linear stress-strain dependence have been investigated. The inelastic deformations with a nonlinear stress-strain dependence influenced by temperature changes have not been considered due to the lack of a consistent model of stress-strain-temperature dependence that can be applied for all types of materials.

Further modeling is required for the inelastic deformations taking into account temperature effects and all the changes in geometry and in material properties of the components of a forming system due to deformation and to the temperature rise. Because the model of inelastic deformation does not lend itself to generalization and is dependent on material and temperature, the further modeling will be more oriented on a specific material and will require more use of numerical methods than of analytical methods. However, the present semi-analytical model may serve as a benchmark to verify more complicated numerical codes. In addition, our model may address some physical issues in further electromagnetic forming experiments [22].

## REFERENCES

[1] C. J. Carpenter, "Surface-integral methods of calculating forces on magnetized iron parts," *Inst. Elect. Eng.*, pp. 19–28, Aug. 1959. Monograph no. 342.

[2] ——, "Distribution of mechanical forces in magnetized material," *Inst. Elect. Eng. Proc.*, vol. 113, no. 4, pp. 719–720, Apr. 1966.

[3] J. V. Byrne, "Ferrofluid hydrostatics according to classical and recent theories of the stresses," *Inst. Elect. Eng. Proc.*, vol. 124, no. 11, pp. 1089–1097, Nov. 1977.

[4] G. W. Carter, "Distribution of mechanical forces in magnetized material," *Inst. Elect. Eng. Proc.*, vol. 112, no. 9, pp. 1771–1777, Sept. 1965.

[5] G. Reyne, J. C. Sabonnadiere, J. L. Coulomb, and P. Brisonneau, "A survey of the main aspects of magnetic forces and mechanical behavior of ferromagnetic materials under magnetization," *IEEE Trans. Magn.*, vol. 23, no. 5, pp. 3765–3767, Sep. 1987.

[6] S. Bobbio, *Electrodynamics of Materials. Forces, Stresses, and Energies in Solids and Fluids*. San Diego, CA: Academic, 2000.

[7] R. M. Fano, L. J. Chu, and R. B. Adler, *Electromagnetic Fields, Energy and Forces*. New York: Wiley, 1960.

[8] L. D. Landau and E. M. Lifschitz, *Electrodynamics of Continuous Media*. Oxford, U.K.: Pergamon, 1960.

[9] P. Penfield and H. A. Haus, *Electrodynamics of Moving Media*. Cambridge, MA: MIT Press, 1967.

[10] T. E. Motoasca, H. Blok, M. D. Verweij, and P. M. van den Berg, "Electromagnetic forming by distributed forces in magnetic and nonmagnetic materials," *IEEE Trans. Magn.*, vol. 40, no. 5, pp. 3319–3330, Sep. 2004.

[11] K. Baines, J. L. Duncan, and W. Johnson, "Electromagnetic metal forming," in *Proc. Inst. Mech. Eng.*, vol. 180, 1965–1966, pp. 93–104.

[12] G. K. Lal and M. J. Hillier, "The electrodynamics of electromagnetic forming," *Int. J. Mech. Sci.*, vol. 10, pp. 491–498, 1968.

[13] C. Fluerasu, "Electromagnetic forming of a tubular conductor," *Rev. Roumaine Sci. Tech., Serie Electrotechnique et Energetique*, vol. 15, pp. 457–488, 1970.

[14] S.T.S. Al-Hassani, J. L. Duncan, and W. Johnson, "On the parameters of magnetic forming process," *J. Mech. Eng. Sci.*, vol. 16, pp. 1–9, 1974.

[15] R. Winkler, *Hochgeschwindigkeitsbearbeitung*. Berlin, Germany: VEB Verlag Technik, 1973, pp. 294–367.

[16] H. Zhang, M. Murata, and H. Suzuki, "Effects of various working conditions on tube bulging by electromagnetic forming," *J. Mater. Process. Technol.*, vol. 48, pp. 113–121, 1995.

[17] S. H. Lee and D. N. Lee, "Finite element analysis of electromagnetic forming for tube expansion," in *Trans. ASME, J. Eng. Mater. Technol.*, vol. 116, Apr. 1994, pp. 250–254.

[18] S. H. Lee and D. N. Lee, "Estimation of the magnetic pressure in tube expansion by electromagnetic forming," *J. Mater. Process. Technol.*, vol. 57, pp. 311–315, 1996.

[19] M. Besbes, Z. Ren, and A. Razek, "A generalized finite element model of magnetostriction phenomena," *IEEE Trans. Magn.*, vol. 37, no. 5, pp. 3324–3328, Sep. 2001.

[20] V. S. Arpaci, *Introduction to Heat Transfer*. Upper Saddle River, NJ: Prentice-Hall, 1999.

[21] D. Iesan and A. Scalia, *Thermoelastic Deformations*. Dordrecht, The Netherlands: Kluwer Academic, 1996.

[22] A. El-Azab, M. Garnich, and A. Kapoor, "Modeling of the electromagnetic forming of sheet metals: State-of-the-art and future needs," *J. Mater. Process. Technol.*, vol. 142, pp. 744–754, Apr. 2003.

**T. Emilia Motoasca** was born in Brasov, Romania, on November 3, 1971. She received the B.S. and M.S. degrees in electrical engineering in 1996 and 1997, respectively, and the B.S. degree in economic sciences in 1997, all from the "Transilvania" University of Brasov. She received the Ph.D. degree in technical sciences from the Delft University of Technology, Delft, The Netherlands, in 2003. Her doctoral research was focused on electrodynamics in deformable media for electromagnetic forming.

From 1997 to 1998 she was a Research Assistant at the "Transilvania" University of Brasov and from 1999 to 2003 she was employed at the Laboratory of Electromagnetic Research, Department of Electrical Engineering, Delft University of Technology. Since November 2003, she has been a Postdoctoral Researcher at the Faculty of Electrical Engineering, Eindhoven University of Technology, Eindhoven, the Netherlands. Her current research interests include analytical and numerical aspects of the theory of electromagnetic waves with applications in medical devices.

**Peter M. van den Berg** was born in Rotterdam, The Netherlands, on November 11, 1943. He received the degree in electrical engineering from the Polytechnical School of Rotterdam in 1964, and the M.Sc. degree in electrical engineering and the Ph.D. degree in technical sciences from the Delft University of Technology, Delft, The Netherlands, in 1968 and 1971, respectively.

From 1967 to 1968, he was a Research Engineer for the Dutch Patent Office. From 1968 to 2003, he was a member of the Scientific Staff of the Electromagnetic Research Group of the Delft University of Technology. During the academic year 1973–1974, he was Visiting Lecturer in the Department of Mathematics, University of Dundee, Scotland, financed by an award from the Niels Stensen Stichting, The Netherlands. During a three-month period in 1980–1981, he was a Visiting Scientist at the Institute of Theoretical Physics, Goteborg, Sweden. He was appointed as a Full Professor at the Delft University of Technology in 1981. During the years of 1988–1994, he also carried out research at the Center of Mathematics of Waves, University of Delaware, USA; these visits have been financed by a NATO award. During the summer periods of 1993–1995, he was a Visiting Scientist at Shell Research B.V., Rijswijk, The Netherlands. Further in 2004 and 2005 he was a Visiting Scientist at Schlumberger-Doll Research, Ridgefield, CT. Since 2003, he has been a Research Professor in the Faculty of Applied Sciences of the Delft University of Technology. His research interest is the efficient computation of field problems using iterative techniques based on error minimization, the computation of fields in strongly inhomogeneous media, and the use of wave phenomena in seismic data processing. His major interest is in an efficient solution of the nonlinear inverse scattering problem.

**Hans Blok** was born in Rotterdam, The Netherlands, on April 14, 1935. He received the degree in electrical engineering from the Polytechnical School of Rotterdam in 1956, and the M.Sc. degree in electrical engineering (cum laude) and the Ph.D. degree in technical sciences (cum laude) from the Delft University of Technology, Delft, The Netherlands, in 1963 and 1970, respectively.

Since 1968, he has been a Member of the Scientific Staff of the Laboratory of Electromagnetic Research, Delft University of Technology. He has done research and lectured in the areas of signal processing, wave propagation, and scattering problems. In 1972 he was appointed Associate Professor ("Reader") at the Delft University of Technology, and in 1980 he became a Full Professor. From 1980 to 1982 he was Dean of the Faculty of Electrical Engineering. During the academic year 1983–1984 he was a visiting scientist at Schlumberger-Doll Research, Ridgefield, CT, where he was involved in modeling of electromagnetic prospecting problems. Since then, he has been visiting scientist at Schlumberger-Doll Research on a regular basis. On and off, he was and is acting head of the Laboratory of Electromagnetic Research. He has been Emeritus Professor since 2000. His current research interests are inverse scattering problems and near-field optics.

**Martin D. Verweij** was born in Alphen aan den Rijn, The Netherlands, in 1961. He received the B.Sc. degree in electrical engineering from the Municipal Polytechnical School, The Hague, The Netherlands, in 1983, and the M.Sc. degree in electrical engineering and the Ph.D. degree in technical sciences from the Delft University of Technology, Delft, The Netherlands, in 1988 and 1992, respectively.

From 1993 to 1997, he was a Research Fellow of the Royal Netherlands Academy of Arts and Sciences. For several months in 1995 and 1997 he was a Visiting Scientist at Schlumberger Cambridge Research, Cambridge, U.K. In 1998 he became an Assistant Professor, and in that same year he became an Associate Professor, both in the Laboratory of Electromagnetic Research of the Delft University of Technology, where he is currently involved in the research and the teaching of the fundamentals of electromagnetic fields and waves. His present research interests are the computational modeling of electromagnetic deformation, nonlinear waves, and nano-optics.

Dr. Verweij is a national member of Commission B (Fields and Waves) of the URSI and a member of the Acoustical Society of America. He has authored or coauthored more than 30 papers in international journals and international conference proceedings.